Desalination and Water Treatment
www.deswater.com

doi: 10.1080/19443994.2015.1137231

57 (2016) 24056–24069
October

Taylor & Francis
Taylor & Francis Group

Novel activated carbon prepared from an agricultural waste, *Stipa tenacissima*, based on $ZnCl_2$ activation—characterization and application to the removal of methylene blue

Abdallah Bouguettoucha[a,*], Abdelbaki Reffas[b], Derradji Chebli[a], Tahar Mekhalif[c], Abdeltif Amrane[d,e]

[a]*Laboratoire de Génie des Procédés Chimiques (LGPC), Faculté de Technologie, Département de Génie des Procédés, Université Ferhat Abbas, Sétif-1, 19000 Sétif, Algeria, Tel./Fax: +213 36 92 51 21; emails: abd_bouguettoucha@yahoo.fr (A. Bouguettoucha), derradji_chebli@yahoo.fr (D. Chebli)*
[b]*Laboratoire de Matériaux Inorganiques (LMI), Faculté de sciences, Université Mohamed Boudiaf – M'sila, M'sila, Algeria, email: Abdelbakireffas@gmail.com*
[c]*Faculté de Science, Département de Chimie, Université de Skikda, Skikda, Algeria, email: smekhalif@yahoo.fr*
[d]*Ecole Nationale Supérieure de Chimie de Rennes, Université de Rennes 1, CNRS, UMR 6226, Avenue du Général Leclerc, CS 50837, 35708, Rennes Cedex 7, Rennes, France, email: abdeltif.amrane@univ-rennes1.fr*
[e]*Université´ Européenne de Bretagne, Bd Laennec, 35000 Rennes, France*

Received 28 May 2015; Accepted 27 December 2015

ABSTRACT

Activated carbon (AC) was prepared by means of a novel physiochemical activation method from low-cost biosorbent, agricultural waste (*Stipa tenacissima* fiber). A two-step pyrolysis was considered instead of a single-step pyrolysis, which involved zinc chloride for the first activation step and a steam mixture of water, CO_2 and acetic acid for the second step. The obtained AC was tested as an adsorbent for the removal of a basic dye, Methylene blue (MB) from aqueous solutions. Batch experiments were conducted to examine the effect of the main parameters, such as the initial MB concentration, the pH, and the kinetic adsorption of this dye. Results showed that a pH value of 7 is favorable for the adsorption of MB. Rate constants of pseudo-first-order, pseudo-second-order, and intraparticle diffusion coefficient were calculated to analyze the dynamic of the adsorption process; they showed that adsorption kinetics followed a pseudo-second-order and an intraparticle diffusion model, while the two straight lines describing experimental data indicated that intraparticle diffusion was not the limiting mechanism for adsorption. Among the tested isotherm models, the Sips isotherm was found to be the most relevant to describe MB adsorption onto both activated and non-ACs with the best maximum adsorption capacity (Q_m), 178.44 and 27.21 mg g^{-1}, respectively. The negative values of ΔG° revealed that the adsorption process was spontaneous. The positive values of ΔH° and ΔS° showed the endothermic nature and an increase in disorder of MB molecules during the adsorption process, respectively.

Keywords: Activated carbon; *Stipa tenacissima*; Characterization; Basic dye; Adsorption

*Corresponding author.

1944-3994/1944-3986 © 2016 Balaban Desalination Publications. All rights reserved.

1. Introduction

Dyes are widely used in industries such as textiles, rubber, paper, plastics, cosmetics etc. Effluents of these industries may therefore contain undesired quantities of these pollutants and hence need to be treated. It is reported that there are around 100,000 commercially available dyes with a production of over 7×10^5 metric tons per year. The presence of coloring material in water system also reduces light penetration and photosynthetic activity due to their content in aromatics, metals, chlorides, etc. Therefore, the treatment of dyes contaminated aquatic systems and improvement of water quality are important topics in the field of environmental technologies [1–4]. From this, it is imperative to remove these substances from waste streams before they are discharged into public waterways. The synthetic origin and complex aromatic structures of dyes make them stable and difficult to be biodegraded [5,6]. Many physical, chemical, and biological methods have been developed to remove dyes, such as coagulation/flocculation, electroflocculation, advanced oxidation, ozonation, membrane filtration, liquid–liquid extraction, electrochemical destruction, ion-exchange, and irradiation [7–11]. However, all these processes have their own limitations; they can appear expensive and not adaptable to a wide range of dye wastewaters [7]. Adsorption is a very effective separation technique and now it is considered to be superior to other techniques for water treatment in terms of investment cost, simplicity of design, ease of operation, and insensitiveness to toxic substances [9,10,12,13]. In this process, the dye species are transferred from the water effluent to a solid phase, leading to decreasing polluted effluent volume [14]. A commonly used adsorbent, activated carbon (AC), has a high capacity for the removal of dyes/organics [15,16]; but some of its disadvantages are its high price and the difficulty to be regenerated inducing an increase of the wastewater treatment cost.

There is therefore a demand for other adsorbents, especially made up of inexpensive material and locally available to allow adsorption processes to become economically viable. In this context, biosorption has emerged as an alternative eco-friendly technology to remove dyes from aqueous solutions. This technology has several advantages, such as simplicity of design, ease of operation, insensitivity to toxic substances, and complete removal of pollutants [1,10]. Biosorption refers to the ability of certain biomaterials to bind and concentrate toxic pollutants from even the most dilute aqueous solutions [1]. In the case of dyes removal, many biosorbents have been reported in the literature recently, such as chitosan [18], fungi [19,20]; algae [17,21], bacteria [4,22], and more recently, low-cost adsorbents [23], ash of *Cassia fistula* seeds [24], rice husk [25], coconut shell and coal ash [26], *Stipa tenassicima* fibers [27], cone of *Pinus brutia* [28], and wild carob [29].

Methylene blue (MB) is a cationic (basic) and water-soluble dye, which has a wide range of coloring applications, such as paper, hair colorant, cottons, wools, and coating for paper stock [30]. It is a cationic (basic) dye which has been known to cause eye irritation, cancer, allergic dermatitis, skin irritation, and even mutation in humans [31,32]. In the present study, AC, prepared from low-cost biosorbent *S. tenacissima* fiber [27] has been used as an adsorbent for the removal of MB from aqueous solutions. The purpose is to optimize the management of this important waste as an adsorbent. The main focus of this study was to evaluate the effects of the main operating parameters, namely pH, initial concentration of MB, and the adsorption kinetic on the adsorption capacity of MB onto this material. Various isotherm models, namely Langmuir [33], Freundlich [34], and Sips [35] were applied to fit equilibrium adsorption data. Furthermore, experimental data were analyzed by means of the pseudo-second-order and intraparticle diffusion models.

2. Materials and methods

2.1. Preparation of the adsorbent

S. tenacissima fibers are prepared as previously described [27]. AC was prepared according to the following four steps:

(1) The first step, namely the carbonization, consisted to put 40 g of fibers in an oven at 300˚C during 8 h.
(2) Pyrolysis: This step was carried out in a small oven in the presence of N_2 at 600˚C for 1 h.
(3) The activation was then done according to two treatments.

The first treatment with $ZnCl_2$, in this step the carbonizer was impregnated by a solution of $ZnCl_2$ at boiling temperature until total vaporization [36].

The second treatment involved CO_2 and H_2O. In a balloon of 100 ml, 10 ml of acetic acid was added and then distilled water until a total volume of 100 ml. The mixture was then heated until boiling, N_2 was then introduced in the mixture, and the vapors flowed in an oven containing the cabonizer at 600˚C during 1 h.

(4) Oxidation: In an Erlenmeyer of 250 ml, 10 ml of a solution of H_2SO_4 (1 M) (ρ = 1.4 kg/m^3) was introduced with 1 g of AC. The solution was then stirred at 300 tr/min on a hot plate, and ammonium persulfate (oxidant) was then added until saturation of the solution, and the carbonizer was added at 30˚C for 24 h. After oxidation, the obtained AC was washed with distilled water [37].

2.2. Characterization

AC prepared form *S. tenacissima* fibers was tested for the adsorption of MB from aqueous solutions.

The pH_{pzc} was determined by the so-called pH drift method. The pH of suspensions of AC and non-activated carbons (NAC) (50 mg) in 50 ml distilled water was adjusted to achieve initial pH values in the range 2–12 with HCl (0.1 M) or NaOH (0.1 M). The suspensions were stirred for 24 h and the final pH was measured and plotted vs. the initial pH. The pH_{pzc} corresponded to the value for which $pH_{final} = pH_{initial}$. The surface acidity was estimated by mixing 0.20 g of AC and NAC with 25 cm^3 of 0.05 M NaOH solution in a closed flask, agitated for 48 h at room temperature. The suspension was separated and the remaining NaOH was titrated with 0.05 M of HCl. The surface alkalinity was measured by titration with 0.05 M of NaOH after incubation for 48 h of 0.20 g of AC and NAC with 0.05 MHCl. The physical and chemical characteristics of the AC and NAC are given in Table 1.

2.3. Preparation of dye solutions and concentration determination

MB, a typical cationic dye (Fig. 1) was selected as an adsorbent. MB dye is a 3,7-bis-(dimethylamino) phenazathionium, namely with the following formula, $C_{16}H_{18}N_3ClS$. MB has a molecular weight of 319.85 g/moL and was obtained from ACROS with 99.99% purity. A stock solution of 50 mg L^{-1} was prepared by dissolving an appropriate amount of MB in a liter of distilled water. The working solutions were prepared by dilution of the stock solution with distilled water to yield the appropriate concentrations. The pH of the solutions was adjusted by addition of either 0.1 M HCl or 0.1 M NaOH solutions, respectively. Before use, all bottles and glassware were beforehand cleaned and then rinsed with distilled water and oven dried at 60˚C. An SP-8001 UV/vis Spectrophotometer of Axiom (Germany, Shimadzu) was used to determine the residual dye concentrations. After withdrawing samples at fixed time intervals and centrifugation, the supernatant was analyzed for residual MB at λ_{max} corresponding to the maximum absorption for the dye solution (λ_{max} = 668 nm). Calibration curve between absorbance and dye concentration was plotted to obtain absorbance–concentration profile.

Table 1
Physical and chemical characteristics of AC developed from *S. tenacissima* fibers

Parameter	Value	
	AC	NAC
BET, surface area (m^2 g^{-1})	451.51	20
Acidity (meq g g^{-1})	12.0	7.5
Basicity (meq g g^{-1})	3.0	4.0
pHpzc	3.24	3.30

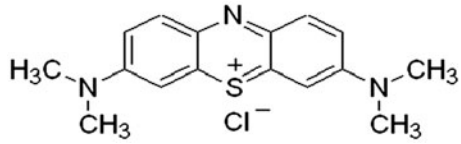

Fig. 1. Molecular structure of methylene blue.

2.4. Adsorption study

The effect of the initial dye concentration was carried out at a given amount of 50 mg of adsorbent, at room temperature (25 ± 2˚C), pH 11, 250 rpm shaking speed, and at different initial concentrations of dye (50, 100, 200 mg L^{-1}) for 500 and 1,000 min for AC and NAC, respectively. Batch experiments of a given amount of adsorbent in 50 mL of dye solutions of a known concentration were carried out.

The amount of dye adsorbed onto AC and NAC at time t, Q_t (mg g^{-1}) was calculated by the following mass balance relationship:

$$Q_t = \frac{(C_0 - C_t)V}{m} \quad (1)$$

The dye removal efficiency was calculated by applying Eq. (2):

$$\eta\,(\%) = \frac{(C_0 - C_e)}{C_0} \times 100 \quad (2)$$

where C_0 is the initial dye concentration (mg L^{-1}), C_e is the concentration of dye at equilibrium (mg L^{-1}), V is the volume of solution, and m is the mass of AC and NAC.

2.5. Equilibrium modeling

Equilibrium data, commonly known as adsorption isotherms, describe how adsorbates interact with adsorbents and hence are critical in optimizing the use of adsorbents and provide information on the capacity of the adsorbent. To analyze AC and NAC interaction with MB, experimental data points were fitted to the Langmuir, Freundlich, and Sips empirical models which are the most frequently used two- and thee-parameter equations in the literature describing the non-linear equilibrium between the pollutant adsorbed on the adsorbent (Q_e) and the pollutant in solution (C_e) at a constant temperature.

The Langmuir isotherm model assumes uniform energies of adsorption onto the adsorbent surfaces. Furthermore, the Langmuir equation is based on the assumption of the existence of monolayer coverage of the adsorbate at the outer surface of the adsorbent where all adsorption sites are identical. The Langmuir equation [33] is given as follows:

$$\frac{Q_e}{Q_m} = \frac{K_L C_e}{1 + K_L C_e} \tag{3}$$

where Q_e is the equilibrium dye concentration on the adsorbent (mg g^{-1}); C_e, the equilibrium dye concentration in solution (mg L^{-1}); Q_m, the monolayer capacity of the adsorbent (mg g^{-1}); and K_L is the Langmuir constant. A non-linear fit was performed by means of the Origin Software in order to obtain the Langmuir model parameters. The parameter statistic "adjusted R^{2}" were also determined to identify the most accurate model to describe experimental results.

The Freundlich isotherm model assumes neither homogeneous site energies nor limited levels of adsorption. The Freundlich model is the earliest known empirical equation and is shown to be consistent with exponential distribution of active centers, characteristic of heterogeneous surfaces [34]:

$$Q_e = K_F C_e^{1/n} \tag{4}$$

where Q_e is the equilibrium dye amount on the adsorbent (mg g^{-1}); C_e, the equilibrium dye concentration in solution (mg L^{-1}); K_F and $1/n$ are empirical constants indicative of adsorption capacity and adsorption intensity, respectively. The Freundlich parameters were obtained by performing a non-linear fit (Origin software).

The Sips isotherm is a combination of the Langmuir and Freundlich isotherms [35]:

$$\frac{Q_e}{Q_{ms}} = \frac{(K_s C_e)^m}{1 + (K_s C_e)^m} \tag{5}$$

where Q_{ms} is the maximum monolayer adsorption (mg g^{-1}), K_s is the Sips constant solution (mg L^{-1}) and m the exponent of the Sips model.

2.5.1. Statistique calculation

The χ^2 test (Eq. (6)) is a statistical test that can be used in determining how well the data obtained from an experimental data matches the expected ones:

$$\chi^2 = \sum \frac{(Q_{exp} - Q_{cal})^2}{Q_{cal}} \tag{6}$$

where Q_{exp} is the equilibrium capacity (mg g^{-1}) obtained from experimental data, and Q_{cal}, is the equilibrium capacity obtained by calculating from the model (mg g^{-1}).

2.6. Kinetic modeling

The study of adsorption dynamics described the solute adsorption rate. This rate controlled the residence time of adsorption at the solid–solution interface. Several kinetic models such as pseudo-first-order, pseudo-second-order, and intraparticle diffusion models were applied to fit experimental data.

2.6.1. Pseudo-first-order model

The pseudo-first-order kinetic model is the first equation for the adsorption of solid/liquid system based on the adsorption capacity. The linear form of the pseudo-first-order equation is given by Eq. (7):

$$\ln(Q_e - Q_t) = \ln Q_e - k_1 t \tag{7}$$

where Q_e (mg g^{-1}) and Q_t (mg g^{-1}) refer to the amount of dye adsorbed at equilibrium and at time t (min), respectively; k_1 (min^{-1}) is the equilibrium rate constant of pseudo-first-order equation. The rate constants are obtained from the straight line plots of ln ($Q_e - Q_t$) against t.

2.6.2. Pseudo-second-order model

The pseudo-second-order model is based on the assumption of chemisorption of the adsorbate on the adsorbent [38]. This model is given by Eq. (8):

$$\frac{t}{Q_t} = \frac{1}{k_2 Q_e^2} + \frac{1}{Q_e} t \quad (8)$$

where k_2 (g mg^{-1} min^{-1}) is the equilibrium rate constant of pseudo-second-order equation. The straight line plots of t/Q_t against t were tested to obtain the rate constant.

2.6.3. Intraparticle diffusion model

Intraparticle diffusion model is commonly used to identify the adsorption mechanism for design purpose. According to Weber and Morris [39], for most adsorption processes, the uptake varies almost proportionally with $t^{1/2}$ rather than with the contact time and can be represented as follows:

$$Q_t = K_{id}\, t^{0.5} + C \quad (9)$$

where Q_t is the amount adsorbed at time t and $t^{0.5}$ is the square root of the time, C is the intercept, and K_{id} (mg g^{-1} min$^{-0.5}$) is the rate constant of intraparticle diffusion.

3. Results and discussion

3.1. IR spectroscopy studies

The infrared spectra of NAC and AC are illustrated in Fig. 2. The absorption band at 3,402 and 3,413 cm^{-1} for AC and NAC, respectively, are characteristic of the stretching vibration of hydrogen-bonded hydroxyl groups (from carboxyls, phenols, or alcohols) and water adsorbed in the ACs (Fig. 2((a) and (b)). The strong band at = 1,443 cm^{-1} observed on the spectrum of NAC can be assigned to the CH_2 bending vibrations and/or to the O–H bending band supported by the existence of phenol in this NAC. However, this band was not observed in the AC. A characteristic absorption of the methyl group (CH bending vibrations in CH_3) was observed at 1,388 cm^{-1} in the AC spectrum.

In the region 900–1,300 cm^{-1}, the AC IR spectrum showed a maximum at 1,089 cm^{-1} and a shoulder at 1,188 cm^{-1}. A maximum at 1,089 cm^{-1} was also observed for NAC but was more pronounced at 1,100 cm^{-1} for this latter. The intensity of this latter band which can be attributed to C–O–C asymmetric stretching was consistent with lactone. The shoulder at 1,188 and 1,166 cm^{-1} for AC and NAC, respectively, which was more pronounced on the AC spectrum than on the NAC spectrum, can be attributed to the

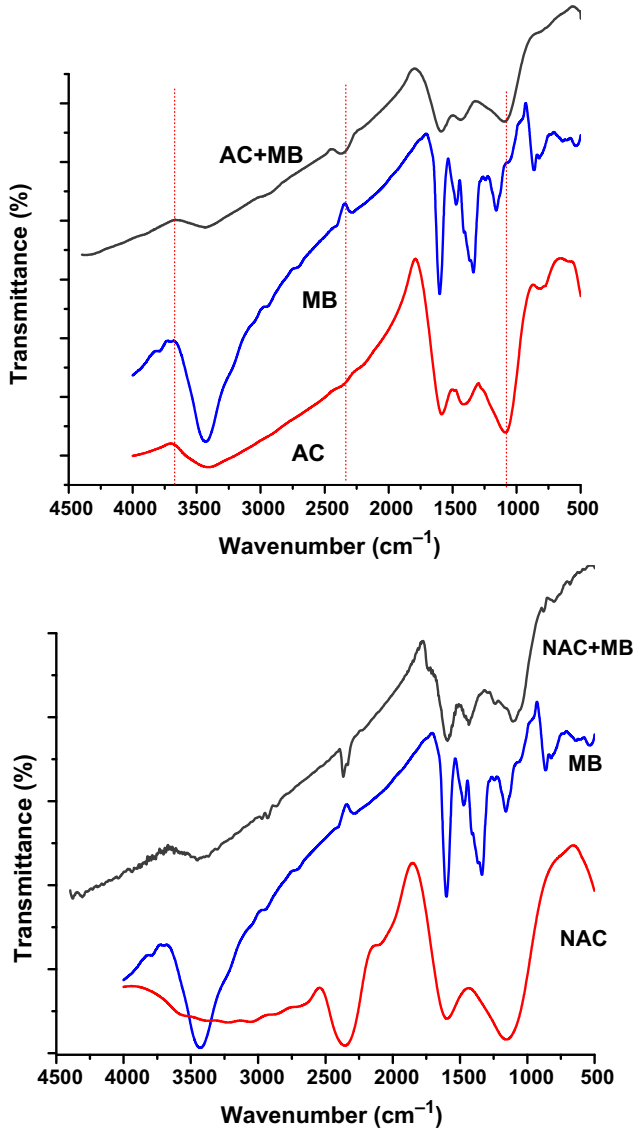

Fig. 2. FT-IR spectra of both NAC and AC before adsorption (a) and after adsorption (b).

C–O stretching (1,188 cm^{-1}) vibration of phenols, acids, ether, and/or esters groups [40]. Aromatic hydrocarbon peak appeared around 1,587 cm^{-1} in both AC and NAC spectra.

To conclude on the IR characterization, the most important changes introduced by the impregnation with a chemical activating agent $ZnCl_2$ are the development of carbonyl groups (shoulders of NAC and AC at 1,166 and 1,188 cm^{-1}) as well as the increase of aromatic hydrocarbon peak (1,587 cm^{-1}).

Moreover, the surface chemistry of AC was modified after adsorption, while it was not the case for NAC as illustrated at the examination of Fig. 2(a) and

(b): a decrease in the intensity of the C–O–C band (at 1,089 cm^{-1}), of the O–H bending band (at 3,402 cm^{-1}) to zero, of the aromatic hydrocarbon peak which appeared around 1,587 cm^{-1} and of the bands γ (C–H) at 801, 669, and 469 cm^{-1}. All these modifications led to an increase of the AC capacity compared with the NAC prepared in the absence of the chemical activating agent, zinc chloride $ZnCl_2$. However, the new band of low intensity which appeared at 2,018 cm^{-1} after MB adsorption and which could be attributed to a υ (MB-AC) constituted the most striking result. As also shown in Fig. 2, the spectra of NAC before and after adsorption of MB displayed a number of adsorption peaks, indicating the active functional groups of NAC. These peak shifts indicated that especially the bonded –OH groups and C=C group played a major role in MB adsorption on NAC [41] The two bands of relatively low intensity which appeared at 1,096 and 1,443 cm^{-1} after MB adsorption and which could be attributed to a υ (MB-NAC) constituted also the most striking result. The peak at 2,349 cm^{-1} shift at 2,360 cm^{-1} indicated also that especially the bonded C=O in COOH groups played a major role in MB adsorption on NAC.

3.2. Scanning electron micrograph analysis

The surface of NAC and AC was observed with scanning electron microscopy Scanning electron micrograph (SEM) (Hitachi S-3000 N SEM), which showed the existence of highly porous surfaces. Fig. 3(a) and (b) on the one hand and Fig. 3(c) and (d) on the other hand shows the SEM photograph of AC and NAC at 5,000× and 10,000× magnifications, respectively. It can be observed that AC has developed more pores than NAC; which however did not displayed a uniform shape. Through scanning electron microscopy (SEM) observation, it was found that AC have a duplex structure, a hollow and high-porous carbon filament (carbon fiber) surrounded by a aggregates of carbon. It can also be seen that although NAC displayed uniform pores, its adsorption capacity was poorer than AC. To account for this observation, it should be noted that adsorption is a surface phenomenon; therefore, smaller adsorbent particle size offers a comparatively larger and more accessible surface area (more pores developed) and hence higher adsorption occurs at equilibrium.

3.3. Effect of the pH

The initial pH of the adsorption medium is an important parameter in the adsorption capacity of organic matter. The pH values (data not shown) show that the adsorption of MB by NAC and AC increased with the alkalinity of the medium and then the optimal pH was found to be 11. The pHpzc for NAC and AC were 3.24 and 3.30, respectively; and thus the medium pH was higher than or equal to pHpzc for both materials. From this, the surface material was negatively charged, increasing the interaction forces between the adsorbent and the cationic dye MB, accounting for the increase of the adsorbed amount with the pH. The adsorbed amount was higher for AC compared to NAC (almost double) because of the effect of the dehydrating agent ($ZnCl_2$).

3.4. Effect of the contact time and the initial dye concentration

Experiments were duplicated and the mean values are depicted in Fig. 4, indicating a considerable influence of the initial MB concentration on its removal. Based on data illustrated in Fig. 4, adsorption equilibrium, Q_e, increased from 42 to 110 mg g^{-1} with increasing initial concentrations from 50 to 200 mg L^{-1}, showing that the initial dye concentration plays an important role in the adsorption capacities of MB onto AC (Fig. 4(b)) and provides an essential driving force for alleviating the mass transfer resistance between the aqueous phase and the solid medium. The adsorption process increases sharply at the initial stage and gradually reduces as equilibrium approaches. This phenomenon can be attributed to the reduction of immediate solute adsorption due to the lack of available open sites for dye adsorption (saturation), which in turn supported film diffusion. The time required to attain this state of equilibrium is termed as equilibrium time (900 min) (see Table 2) [42].

An opposite behavior was found with NAC (Fig. 4(a)) as adsorbent. This may be due to a phenomenon of attraction and repulsion of the molecules of MB and the surface function located at the surface of the untreated material and/or to the dimensions of the pore. The adsorption equilibrium, Q_e, decreased from 12.2 to 9.4 mg g^{-1} with an increase in the initial concentration from 50 to 200 mg L^{-1}, respectively. The obtained data presented in Table 2 show the increase of percentage removal from 75.5 to 93.9% in the case of NAC, and from 16.0 to 45.0% for AC, with the increase in the initial dye concentration.

3.5. Isotherm analysis

A correct mathematical description of equilibrium adsorption capacity is indispensable for reliable

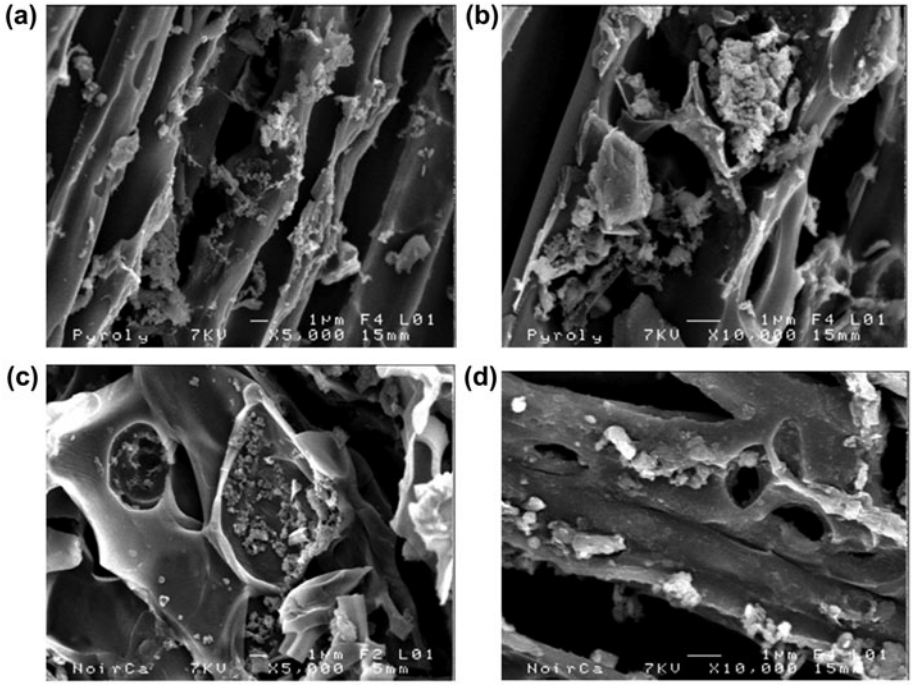

Fig. 3. SEM images of for both NAC (c, d) and AC (a, b) before adsorption.

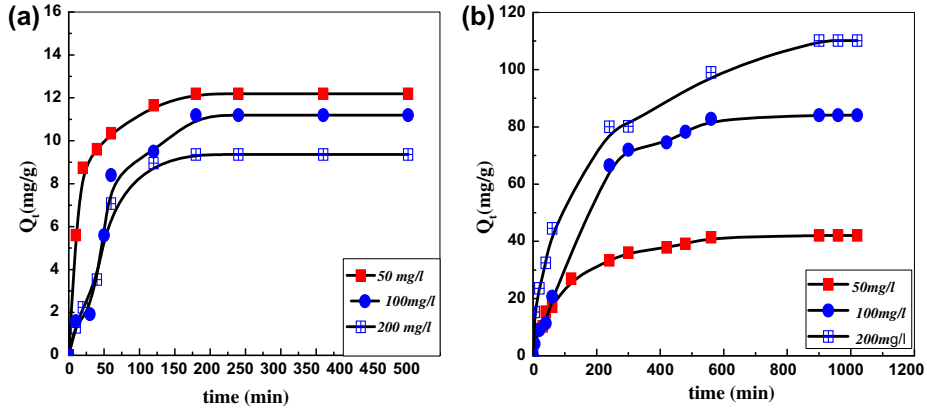

Fig. 4. Effect of the contact time and the initial MB concentration on the adsorption capacity of MB onto both: (a) NAC and (b) AC. (T = 25℃, agitation speed = 200 rpm, pH 11).

prediction of adsorption parameters and quantitative comparison of adsorption behavior for different adsorbent systems (or for varied experimental conditions) within any given system. In order to optimize the design of an adsorption system, it is important to establish the most appropriate correlation for the equilibrium curve. Several equilibrium adsorption isotherm models are available, and the most common ones are the mono-layer adsorption developed by Langmuir [33], the multi-layer adsorption of Freundlich [34], and the Sips isotherm [35]. Experimental data of MB adsorption onto AC and NAC were fitted to the isotherm models using Origin software and the graphical representations of these models are presented in Fig. 5, and all constants are collected in Table 2. The representations of experimental data by all model equations resulted in non-linear curves with R^2 values, tabulated in Table 3. It can be seen from the correlation coefficients of the analyzed isotherms that the Sips model yielded to a better fit of experimental equilibrium data than the other isotherms (Table 3). These results suggest that the adsorption process of

Table 2
Influence of different parameters for the adsorption for the MB on NAC and AC

Adsrobent	Parameters	Initial dye concentration (mg L^{-1})		
		50	100	200
NAC	Q_e (mg g^{-1})	12.5	11.25	9.4
	η (%)	75.5	87.75	93.86
	t_e (min)	180	180	180
AC	Q_e (mg g^{-1})	42	84.4	110
	η (%)	16	15.6	45
	t_e (min)	900	900	900

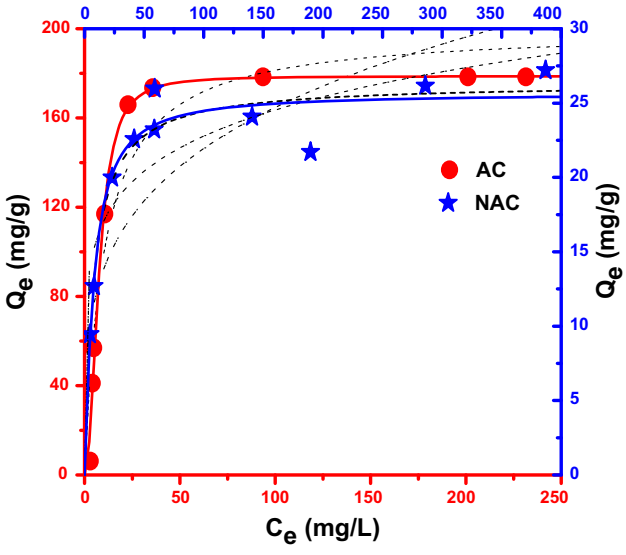

Fig. 5. Experimental (symbols) and calculated isotherm data (lines) for MB adsorption onto both, NAC (top *X* and right *Y*) and AC, Dash line: Langmuir; Dash Dot line: Freundlich; Bold: Sips. (T = 25°C, agitation speed = 200 rpm, pH 11).

the MB dye follows a combination of the Freundlich and Langmuir models: diffused adsorption at low dye concentration, and a mono-molecular adsorption with a saturation value at high dye concentrations. Maximum adsorption capacities given by the Sips adsorption isotherm were 25.60 and 178.75 mg g^{-1} for NAC and AC respectively, showing that AC was more effective than a commercial AC such as CGAC120 [43]. This data indicates that AC can be considered a promising material for the removal of MB dye from aqueous solutions. It should however be observed that the statistical analysis confirms that the Sips model is the most appropriate to describe experimental data, especially the results obtained using AC (Table 4). The

Table 3
Freundlich, Langmuir and Sips constants for the adsorption of MB onto both AC and NAC

Model Parameters	Freundlich		Langmuir		Sips	
	NAC	AC	NAC	AC	NAC	AC
K_f (mg g^{-1})	11.0	51.5	–	–	–	–
n_f	6.33	3.96	–	–	–	–
Q_m (mg g^{-1})	–	–	26.33	199.9	–	–
K_L (mg g^{-1})	–	–	0.13	0.10	–	–
Q_{mS} (mg g^{-1})	–	–	–	–	25.67	178.75
$K_s \times 10^2$	–	–	–	–	0.13	0.13
m	–	–	–	–	1.17	2.20
R^2	0.70	0.64	0.92	0.90	**0.90**	**0.987**
χ^2	1.48	50.70	0.95	9.48	**0.87**	**0.29**

Notes: The values were highlighted in bold in order to illustrate the best fitting model.

comparison of maximum adsorption capacity of some dyes onto various adsorbents is presented in Table 4, showing that AC can be considered as a promising material for the removal of cationic dyes, even compared to some other low-cost adsorbents and ACs previously recommended for the removal of MB from aqueous solutions. Indeed, except NaOH-modified rejected tea, it gives the best maximum adsorption capacity.

3.6. Kinetic models

Generally, three steps are involved during the process of adsorption by porous-adsorbent particles: external mass transfer, intraparticle transport, and chemisorption. For both adsorbents, AC and NAC, adsorption kinetics appeared to be accurately fitted by the pseudo-second-order and the intraparticle diffusion models (Table 5), while the pseudo-first-order model (Fig. 6) did not result in an accurate description of experimental data, owing to correlation coefficients (R^2) below 0.90 (Table 4). This suggests that the sorption of MB onto NAC and AC does not follow the pseudo-first-order sorption rate expression. In addition to the high R^2 values (>0.99 for all tested conditions), the Q_e values estimated from the pseudo-second-order kinetic model were also in agreement with experimental data (Table 5) at all tested concentrations (Fig. 7). The results suggested that boundary layer resistance was not the rate-limiting step since dye adsorption followed pseudo-second-order kinetics [48]. The above results suggest that the pseudo-second-order kinetic model could be used to predict the amounts of dye taken up at different contact time intervals and at equilibrium.

Table 4
Comparison of the maximum adsorption (Q_m) of MB onto various adsorbents

Adsorbents	Q_m (mg g^{-1})	Refs.
NaOH-modified rejected tea	242.1	[44]
Actived carbon from *S. tenacissima fiber*	178.75	This work
Macauba palm cake (in nature)	27.75	[45]
Macauba palm cake (treated)	33.06	[45]
Rice husk	8.7	[46]
Coir pith activated carbon	5.87	[47]
S. tenacissima (native)	5.35	[27]

Table 5
Kinetics parameters for MB biosorption onto both AC and NAC at different concentrations. ($T = 25 \pm 2$°C, pH 11)

Models			Parameters	Concentration (mg L^{-1})		
				50	100	200
Pseudo-first-order	AC		$Q_{e,exp}$ (mg g^{-1})	42.05	84.1	110.13
			$Q_{e1,cal}$ (mg g^{-1})	37.33	89.46	93.03
			k_1 (1/min)	0.006	0.026	0.016
			R_1^2	0.95	0.96	0.88
	NAC		$Q_{e,exp}$ (mg g^{-1})	12.19	9.36	11.19
			$Q_{e1,cal}$ (mg g^{-1})	8.01	11.65	11.6
			k_1 (1/min)	0.023	0.01	0.026
			R_1^2	0.92	0.88	0.88
Pseudo-second-order	AC		$Q_{e,exp}$ (mg g^{-1})	42.05	84.1	110.13
			$Q_{e2,cal}$ (mg g^{-1})	46,04	93.05	117.64
			$K_2 \times 10^5$ (g/mg min)	0.26	11	9.22
			R_2^2	0.995	0.997	0.987
	NAC		$Q_{e,exp}$ (mg g^{-1})	12.19	9.36	11.19
			$Q_{e2,cal}$ (mg g^{-1})	12.52	10.86	12.23
			$K_2 \times 10^3$ (g/mg min)	8.01	1.7	2.38
			R_2^2	0.999	0.976	0.990
Intraparticle diffusion	AC	Step 1	K_{id} (mg g^{-1} $min^{0.5}$)	1.096	1.8	3.42
			C (mg g^{-1})	15.76	39.16	21.17
			R_{id}^2	0.96	0.95	0.97
		Step 2	K_{id} (mg g^{-1} $min^{0.5}$)	0	0	0
			C (mg g^{-1})	42.05	84.1	110.13
			R_{id}^2	1	1	1
	NAC	Step 1	K_{id} (mg g^{-1} $min^{0.5}$)	0.39	0.41	0.48
			C (mg g^{-1})	7.14	4.04	4.51
			R_{id}^2	0.98	0.98	0.95
		Step 2	K_{id} (mg g^{-1} $min^{0.5}$)	0	0	0
			C (mg g^{-1})	12.9	9.36	11.19
			R_{id}^2	1	1	1

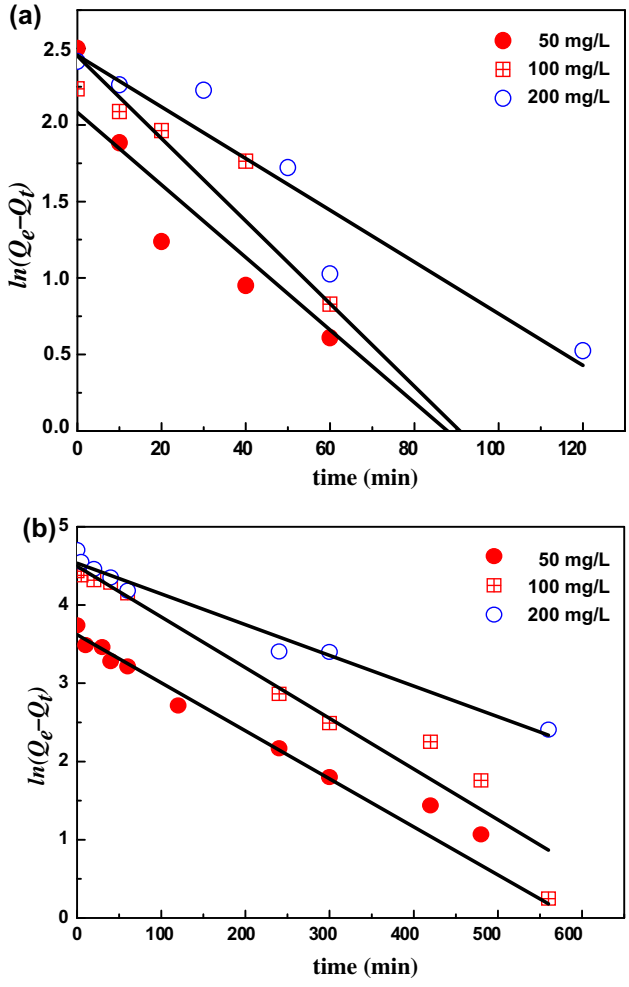

Fig. 6. The fitting of experimental data by means of the pseudo-first-order kinetic model for MB adsorption onto both (a) NAC and (b) AC. At various concentrations (T = 25°C, agitation speed = 200 rpm, pH 11).

The intraparticle diffusion model could be used to investigate the mass transfer mechanism in the dye-activated carbon system. The intercept gives an idea about the thickness of the boundary layer, i.e. the higher is the intercept value the greater is the boundary layer effect [49]. Linear portions of the intraparticle diffusion plots are displayed in Fig. 8 and the corresponding parameters are summarized in Table 4. If the value of C is zero, then the rate of adsorption is controlled by intraparticle diffusion for the entire adsorption period [50]. As observed, irrespective of the considered concentration, the intraparticle diffusion of MB within biomass occurred in two steps. The first straight portion could be attributed to macropore diffusion (step 1), namely the transport of dye molecules from the bulk solution to the surface of the adsorbent, and the second linear portion could be attributed to micropore diffusion (step 2), namely the binding of the dye molecules on the active sites of the adsorbent. From the above results, it is clear that intraparticle diffusion was not the only rate limiting mechanism for the adsorption of MB onto AC and NAC. This kind of multi-linearity in the shape of the intraparticle diffusion plot has also been observed by Waranusantigul et al. [50] and Ofomaja et al. [51].

3.7. Thermodynamic analysis

The thermodynamic parameters reflect the feasibility and the spontaneous nature of a biosorption process. Parameters such as the free energy change (ΔG), the enthalpy change (ΔH), and the entropy change (ΔS) can be estimated using equilibrium constants varying with temperature. The free energy change of the adsorption reaction is given using Eq. (10) as reported by Milonjic [35] and Reffas et al. [29]:

$$\Delta G^{\circ} = -RT \ln(\rho K_c) \tag{10}$$

where ΔG° is the free energy change (kJ mol^{-1}), R the universal gas constant (8.314 J mol^{-1} K^{-1}), T the absolute temperature (K), K_c the thermodynamic equilibrium constant (L g^{-1}) (Eq. (12)), and ρ the water density (g L^{-1}). ΔH° and ΔS° values of the biosorption process were calculated from the Van't Hoff Eq. (11):

$$\ln(\rho K_c) = -\frac{\Delta H^{\circ}}{RT} + \frac{\Delta S^{\circ}}{R} \tag{11}$$

$$K_c = \frac{Q_e}{C_e} \tag{12}$$

ΔH and ΔS can be then deduced from the slope ($\Delta H/R$) and the intercept ($\Delta S/R$) of the plot of $\ln(\rho K_c)$ vs. $1/T$. The calculated thermodynamic parameters are given in Table 6.

In general, the change in free energy for physisorption is between −20 and 0 kJ mol^{-1} and in a range of –80 to −400 kJ mol^{-1} for chemisorption [52]. The result obtained, about −20 kJ mol^{-1} for all tested temperatures, were characteristics of a spontaneous physisorption process; it was in agreement with the high impact of the temperature on MB adsorption. The negative values of ΔG° revealed that the adsorption process was spontaneous. The positive values of ΔH° and ΔS° showed the endothermic nature and an increase in disorder of MB molecules during the adsorption process, respectively.

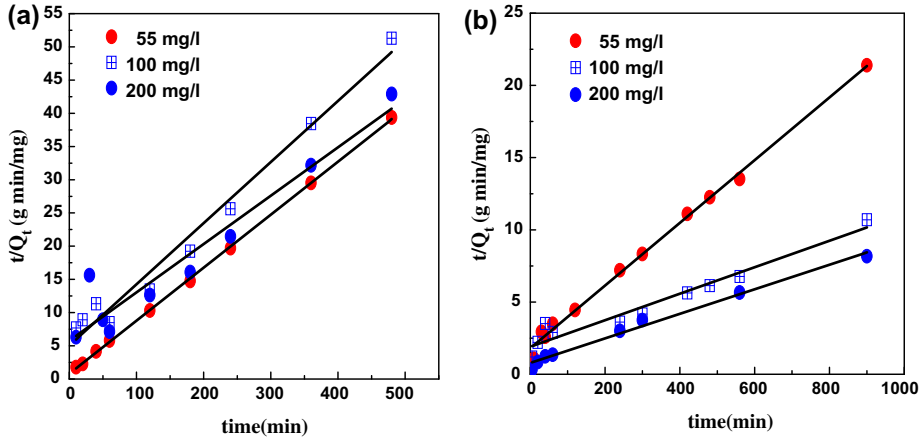

Fig. 7. The fitting of experimental data by means of the pseudo-second-order kinetic model for MB adsorption onto both (a) NAC and (b) AC. At various concentrations (T = 25℃, agitation speed = 200 rpm, pH 11).

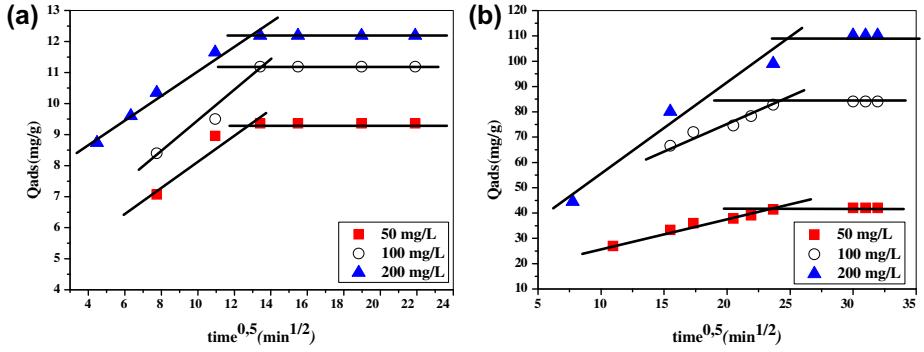

Fig. 8. Intraparticle diffusion kinetic plots for adsorption of MB onto both, (a) NAC and (b) AC. At various concentrations (T = 25℃, agitation speed = 200 rpm, pH 11).

Table 6
Thermodynamic parameters for the adsorption of MB on NAC and AC

	Temperature (K)	ΔH° (kJ/mol)	ΔS° (J/mol K)	ΔG° (kJ/mol)
NAC	297			–15.31
	306	46.33	207.55	–17.18
	316			–19.25
	325			–21.12
AC	297			–18.01
	306	56.36	250.4	–20.26
	316			–22.76
	325			–25.27

3.8. Proposed mechanism of adsorption

Understanding the mechanism of cationic dye adsorption on solid AC and NAC surfaces is essential for an effective removal of dyes from textile wastewaters. The mechanisms of the dye adsorption onto AC and NAC were investigated by using FTIR technique. The AC and NAC surface contains hydroxide groups, which are very reactive groups, which can react with many polar organic compounds and various functional groups. AC and NAC have variable charges that result from the adsorption of ions from the solution, such as H^+ or OH^-. For pH values below the

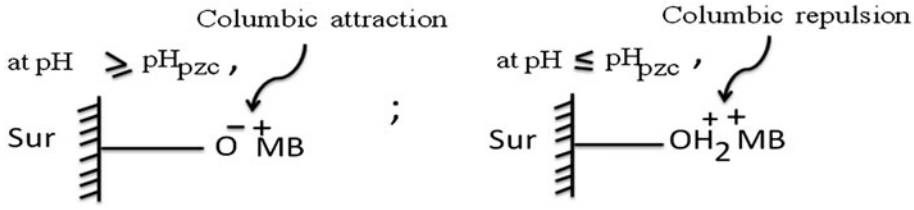

Fig. 9. Schematic representation for possible adsorption mechanism of MB onto AC and NAC at pH ≥ pHpzc and pH ≤ pHpzc.

point of zero charge (Sur—OH + H_3O^+ → Sur —OH_2^+ + H_2O) and for pH values above the point of zero charge (Sur—OH + OH^- → Sur—O^- + H_2O). FTIR offers some indication about the ability of this dye to react with hydroxide groups of the surface of AC and NAC. Fig. 2 shows that when the dye adsorbed on AC and NAC, a decrease in the intensity of the O–H bending band (at 3,402 cm^{-1}) to zero for AC and the peak shifts in the NAC spectra indicated that especially the bonded –OH groups played a major role in MB adsorption on NAC. According to the FTIR spectra and the pH dependency of the adsorption of methylene blue (MB), there was an electrostatic (columbic) repulsion between MB and the positive charge on the surface of AC and NAC at pH below 3 (i.e. pH ≤ 3) (Sur—OH_2^+ + MB); while for pH values above 3 (pH ≥ 3), there was an electrostatic (columbic) attraction between MB and the negative charge on the surface of AC and NAC, leading to an increase of dye removal. Consequently, the mechanism proposed can be illustrated in Fig. 9.

4. Conclusion

The literature dealing with the use of the considered physiochemical activation method in the production of AC remained scarce. In this study, *S. tenacissima* fibers have been considered to prepare AC by this method and a cationic dye was used as a model compound.

An increase in the surface area was observed when the activation took place with zinc chloride solution, which was therefore selected. This study shows that a steam of the mixture, water, CO_2, and acetic acid, was a better activating agent compared to conventional processes; a higher reactivity was shown with acidic steam leading to acidic characteristics as shown through the pHpzc and surface properties.

This activation method appeared to be an easy way to promote the introduction of functional groups (ex: COOH) on the surface of AC; the oxidation was carried out with a solution of acetic acid as described in the experimental protocol. The obtained activation led to a higher oxygen (acidic) content, 12 and 7.5 meq g^{-1} for AC and NAC, and a surface area up to 541.5 m^2 g^{-1} was obtained. This study proved that the product quality of two-step pyrolysis was better compared to the single step pyrolysis.

Experimental data were found to follow a Sips isotherm model. Batch studies showed that a simple model such as pseudo-second-order kinetic equation can adequately predict the adsorption of CR onto both NAC and AC at all studied concentrations. These results imply that chemisorption mechanism may play an important role in dye adsorption. Kinetic study also revealed that intraparticle diffusion was not the limiting step for adsorption. The negative values of ΔG° revealed that the adsorption process was spontaneous. The positive values of ΔH° and ΔS° showed the endothermic nature and an increase in disorder of MB molecules during the adsorption process, respectively

References

[1] Z. Aksu, Application of biosorption for the removal of organic pollutants: A review, Process Biochem. 40 (2005) 997–1026.
[2] S. Dawood, T.K. Sen, Removal of anionic dye Congo red from aqueous solution by raw pine and acid-treated pine cone powder as adsorbent: Equilibrium, thermodynamic, kinetics, mechanism and process design, Water Res. 46 (2012) 1933–1946.
[3] F. Deniz, S.D. Saygideger, Equilibrium, kinetic and thermodynamic studies of Acid Orange 52 dye biosorption by *Paulownia tomentosa Steud*. leaf powder as a low-cost natural biosorbent, Bioresour. Technol. 101 (2010) 5137–5143.
[4] Y. Yang, G. Wang, B. Wang, Z. Li, X. Jia, Q. Zhou, Y. Zhao, Biosorption of Acid Black 172 and Congo Red from aqueous solution by nonviable *Penicillium* YW 01: Kinetic study, equilibrium isotherm and artificial neural network modeling, Bioresour. Technol. 102 (2011) 828–834.
[5] C.A. Fewson, Biodegradation of xenobiotic and other persistent compounds: The causes of recalcitrance, Trends Biotechnol. 6 (1998) 148–153.

[6] S. Seshadri, P.L. Bishop, A.M. Agha, Anaerobic/aerobic treatment of selected azo dyes in wastewater, Waste Manage. 14 (1994) 127–137.
[7] A. Srinivasan, T. Viraraghavan, Decolorization of dye wastewaters by biosorbents: A review, J. Environ. Manage. 91 (2010) 1915–1929.
[8] M. Ghaedi, A. Hassanzadeh, S. NasiriKokhdan, Multi-walled carbon nanotubes as adsorbents for the kinetic and equilibrium study of the removal of alizarin red S and morin, J. Chem. Eng. Data 56 (2011) 2511–2520.
[9] Z. Yao, L. Wang, J. Qi, Biosorption of methylene blue from aqueous solution using a bioenergy forest waste: *Xanthocerassorbifolia* seed coat, Clean 37 (2009) 642–648.
[10] M.M. Abd EI-Latif, A.M. Ibrahim, M.F. EI-Kady, Adsorption equilibrium, kinetics and thermodynamics of methylene blue from aqueous solutions using biopolymer oak sawdust composite, J. Am. Sci. 6 (2010) 267–283.
[11] V. Vimonses, S. Lei, B. Jin, C.W.K. Chow, C. Saint, Kinetic study and equilibrium isotherm analysis of Congo Red adsorption by clay materials, Chem. Eng. J. 148 (2009) 354–364.
[12] T.K. Sen, S. Afroze, H.M. Ang, Equilibrium, kinetics and mechanism of removal of methylene blue from aqueous solution by adsorption onto pine cone biomass of *Pinus radiate*, Water Air Soil Pollut. 218 (2011) 499–515.
[13] M. Mohammad, S. Maitra, N. Ahmad, A. Bustam, T.K. Sen, B.K. Dutta, Metal ion removal from aqueous solution using physic seed hull, J. Hazard. Mater. 179 (2010) 363–372.
[14] M. Ghaedi, J. Tashkhourian, A.A. Pebdani, B. Sadeghian, F.N. Ana, Equilibrium, kinetic and thermodynamic study of removal of reactive orange 12 on platinum nanoparticle loaded on activated carbon as novel adsorbent, Korean J. Chem. Eng. 28 (2011) 2255–2261.
[15] Y.C. Sharma, Uma, Optimization of parameters for adsorption of methylene blue on a low-cost activated carbon, J. Chem. Eng. Data 55 (2010) 435–439.
[16] S. Wang, Z.H. Zhu, A. Coomes, F. Haghseresht, G.Q. Lu, The physical and surface chemical characteristics of activated carbons and the adsorption of methylene blue from wastewater, J. Colloid Interface Sci. 284 (2005) 440–446.
[17] Z. Aksu, S. Tezer, Biosorption of reactive dyes on the green alga *Chlorella vulgaris*, Process Biochem. 40 (2005) 1347–1361.
[18] G.L. Dotto, L.A.A. Pinto, Adsorption of food dyes onto chitosan: Optimization process and kinetic, Carbohydr. Polym. 84 (2011) 231–238.
[19] R. Patel, S. Suresh, Kinetic and equilibrium studies on the biosorption of reactive black 5 dye by *Aspergillus foetidus*, Bioresour. Technol. 99 (2008) 51–58.
[20] M.E. Russo, F. Di Natale, V. Prigione, V. Tigini, A. Marzocchella, G.C. Varese, Adsorption of acid dyes on fungal biomass: Equilibrium and kinetics characterization, Chem. Eng. J. 162 (2010) 537–545.
[21] A. Çelekli, F. Geyik, Artificial neural networks (ANN) approach for modeling of removal of Lanaset Red G on Chara contraria, Bioresour. Technol. 102 (2011) 5634–5638.
[22] G.L. Dotto, E.C. Lima, L.A.A. Pinto, Biosorption of food dyes onto *Spirulina platensis* nanoparticles: Equilibrium isotherm and thermodynamic analysis, Bioresour. Technol. 103 (2012) 123–130.
[23] M.A. Mohammed, A. Shitu, A. Ibrahim, Removal of methylene blue using low cost adsorbent: A review, Res. J. Chem. Sci. 4(1) (2014) 91–102.
[24] H. Kaur, A. Thakur, Adsorption of Congo red dye from aqueous solution onto Ash of *Cassia Fistula* seeds: Kinetic and Thermodynamic Studies, Chem. Sci. Rev. Lett. 3(11) (2014) 159–169.
[25] B. Ramaraju, P. Manoj Kumar Reddy, C. Subrahmanyam, C. Subrahmanyam, Low cost adsorbents from agricultural waste for removal of dyes, Environ. Progress Sustainable Energy 33(1) (2014) 38–46.
[26] C.R. Ramakrishnaiahand, D.N. Arpitha, Removal of colour from textile effluent by adsorption using low cost adsorbents, Int. Res. J. Pure Appl. Chem. 4(5) (2014) 568–577.
[27] D. Chebli, A. Bouguettoucha, T. Mekhalef, S. Nacef, A. Amrane, Valorization of an agricultural waste, *Stipa tenassicima* fibers, by biosorption of an anionic azo dye, Congo red, Desalin. Water Treat. 54 (2015) 245–254.
[28] A. Bouguettoucha, D. Chebli, T. Mekhalef, A. Noui, A. Amrane, The use of a forest waste biomass, cone of *Pinus brutia* for the removal of an anionic azo dye Congo red from aqueous medium, Desalin. Water Treat. 55 (2015) 1956–1965.
[29] A. Reffas, A. Bouguettoucha, D. Chebli, A. Amrane, Adsorption of ethyl violet dye in aqueous solution by forest wastes, wild carob, Desalin. Water Treat. doi: 10.1080/19443994.2015.1031707
[30] V. Vadivelan, K. Vasanth, Equilibrium, kinetics, mechanism, and process design for the sorption of methylene blue onto rice husk, J. Colloid Interface Sci. 286(1) (2005) 90–100.
[31] K.G. Bhattacharyya, A. Sharma, *Azadirachta indica* leaf powder as an effective biosorbent for dyes: A case study with aqueous Congo Red solutions, J. Environ. Manage. 71(3) (2004) 217–229.
[32] R. Caritá, M.A. Marin-Morales, Induction of chromosome aberrations in the Allium cepa test system caused by the exposure of seeds to industrial effluents contaminated with azo dyes, Chemosphere 72 (2008) 722–725.
[33] I. Langmuir, The adsorption of gases on plane surfaces of glass, mica and platinum, J. Am. Chem. Soc. 40 (1918) 1361–1403.
[34] H.M.F. Freundlich, Ober dies adsorption in Losungen (About adsorption in solution), Z. Phys. Chem. 57 (1906) 385–470.
[35] S.K. Milonjic, A consideration of the correct calculation of thermodynamic parameters of adsorption, J. Serbian Chem. Soc. 72 (2007) 1363–1367.
[36] A.H. Abdullah, A. Kassim, Z. Zainal, M.Z. Hussien, D. Kuang, F. Ahmad, O.S. Wooi, Preparation and characterization of activated carbon from gelam wood bark (*Melaleuca cajuputi*), Malays. J. Anal. Sci. 7(1) (2001) 65–68
[37] N. Li, X. Ma, Q. Zha, K. Kim, Y. Chen, C. Song, Maximizing the number of oxygen-containing functional groups on activated carbon by using ammonium persulfate and improving the temperature-programmed desorption characterization of carbon surface chemistry, Carbon 49(15) (2011) 5002–5013.

[38] V.C. Srivastava, I.D. Mall, I.M. Mishra, Adsorption of toxic metal ions onto activated carbon, Chem. Eng. Process. Process Intensif. 47 (2008) 1269–1280.
[39] W.J. Weber, J.C. Morris, Equilibrium and capacities for adsorption on carbon, J. Sanit. Eng. Div. ASCE 89 (1963) 31–60.
[40] J. Coates, Interpretation of infrared spectra, a practical approach, in: R.A. Meyers (Ed.), Encyclopedia of Chemistry, Chichester John Wiley & Sons Ltd, Chichester, 2000, pp. 10815–11037.
[41] E. Malkoc, Y. Nuhoglu, Y. Abali, Cr(VI) adsorption by waste acorn of *Quercus ithaburensis* in fixed beds: Prediction of breakthrough curves, Chem. Eng. J. 119(1) (2006) 61–68.
[42] S. Yuan, Y. Li, Q. Zhang, H. Wang, ZnO nanorods decorated calcined Mg–Al layered double hydroxides as photocatalysts with a high adsorptive capacity, Colloids Surf., A: Physicochem. Eng. Aspects 348(1–3) (2009) 76–81.
[43] A. Reffas, V. Bernardet, B. David, L. Reinert, M.B. Lehocine, M. Dubois, Carbons prepared from coffee grounds by H_3PO_4 activation: Characterization and adsorption of methylene blue and Nylosan Red N-2RBL, J. Hazard. Mater. 175(1–3) (2010) 779–788.
[44] N. Nasuha, B.H. Hameed, Adsorption of methylene blue from aqueous solution onto NaOH-modified rejected tea, Chem. Eng. J. 166 (2011) 783–786.
[45] T. Akar, B. Anilan, A. Gorgulu, S.T. Akar, Assessment of cationic dye biosorption characteristics of untreated and non-conventional biomass: *Pyracantha coccinea* berries, J. Hazard. Mater. 168 (2009) 1302–1309.
[46] M.-C. Shih, Kinetics of the batch adsorption of methylene blue from aqueous solutions onto rice husk: Effect of acid-modified process and dye concentration, Desalin. Water Treat. 37 (2012) 200–214.
[47] S.S. Vieira, Z.M. Magriotis, N.A.V. Santos, M. das Gracas Cardoso, A.A. Saczk, Macauba palm (*Acrocomia aculeata*) cake from biodiesel processing: An efficient and low cost substrate for the adsorption of dyes, Chem. Eng. J. 183 (2012) 152–161.
[48] X.J. Xiong, X.J. Meng, T.L. Zheng, Biosorption of C.I. Direct Blue 199 from aqueous solution by nonviable *Aspergillus niger*, J. Hazard. Mater. 175 (2010) 241–246.
[49] M.S. Chiou, H.Y. Li, Adsorption behavior of reactive dye in aqueous solution on chemical cross-linked chitosan beads, Chemosphere 50 (2003) 1095–1105.
[50] P. Waranusantigul, P. Pokethitiyook, M. Kruatrachue, E.S. Upatham, Kinetics of basic dye (methylene blue) biosorption by giant duckweed (*Spirodela polyrrhiza*) Environ, Environ. Pollut. 125(3) (2003) 385–392.
[51] A.E. Ofomaja, Kinetics and mechanism of methylene blue sorption onto palm kernel fibre, Process Biochem. 42 (2007) 16–24.
[52] D. Myers, Surfaces, Interfaces, and Colloids: Principles and Applications (second ed.), John Wiley & Sons, Inc., New York, NY, 1999 187–190.